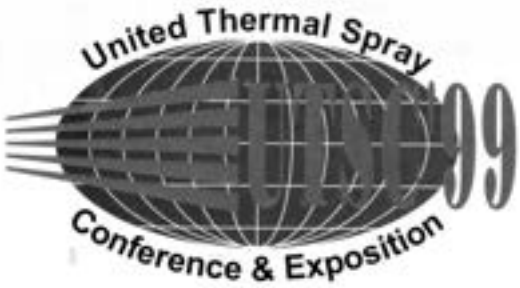

United Thermal Spray Conference

Düsseldorf
17. bis 19. März 1999

Tagungsband Conference Proceedings

Herausgeber / Editors
E. Lugscheider
P. A. Kammer

Mathematical modeling of splat formation at off-normal angles in thermal spray

H. Fukanuma, Toda City/J, and C.-J. Li, Xian/TJ

Mathematische Modellierung der Spritzerausbildung beim thermischen Spritzen abweichend von der Bauteilnormalen

In dieser Studie wird ein Modell für die Spritzerbildung bei anormalen Spritzwinkeln beim thermischen Spritzen vorgeschlagen. Es zeigt sich, daß die Spritzer elliptisch werden, wenn die Spritzwinkel anormal sind, und daß sich die Ellipse dehnt, je mehr der Winkel von der Lotrechten abweicht. Mit dem Modell wurden Versuchsergebnisse der Spritzerdehnung bei anormalen Aufprallwinkeln verglichen.

1 Introduction

This paper aims to clarify the molten particle deformation in off-normal angle impingement under certain physical and mathematical assumptions. The splat formation at off-normal angles in thermal spray is not well understood, although there have been some qualitative investigations of splat morphology and the characteristics of sprayed layers in off-normal angle spray. Montavan et al reported that the elongation ratio increased from approximately 1 to 2 when the spray angle changed from 90° to 30°. However, the average equivalent splat diameter was not significantly influenced by the changes of spray angle [1]. In another study, Montavan and Coddet showed that a lower spray angle resulted in a greater slope of the splat thickness [2]. Smith investigated the spray angle dependence of deposition efficiency, surface roughness and porosity for several spray materials [3]. That particular study is practical and useful, however it did not include information about how the splat morphology depended on spray angle. On the other hand, Sobolev reported a mathematical flattening model taking into account impact angles [4]. However, the model is treated under the assumption that splat circularity is held between 45° and 90°. The theory does not include an analysis of splat shapes whose circularity decreases when the spray angle changes from the perpendicular.

The relationship between the splat elongation ratio and spray angles is found in this paper under the assumptions that (i) the splats are elliptic at off-normal spray angles, (ii) a molten particle which impinges onto a substrate at declined angle moves away from the impact point along the substrate and (iii) the intersection of the substrate surface and a vertical line through the particle center is the second focal point of the ellipse, if the impact point is the first focal point.

2 Modeling

A molten particle whose diameter is d_0 impinges onto a flat smooth substrate at velocity v_0 and impact angle φ. Then, a radial flow begins to spread from the particle impingement point. The splat thickness h is assumed a constant during the flattening. When the impinging angle is φ, the particle velocity components perpendicular and parallel to the substrate at impact are $v_0 \sin\varphi$ and $v_0 \cos\varphi$, respectively. The particle moves towards the substrate and concurrently moves along the substrate. The splat is a circle at the very moment of impact, then the splat becomes elliptic. The oval shape is growing elongated and larger with elapsed time t as shown in **Fig. 1**. The impact point of the particle is one of the two focal points in the ellipse. The other focal point moves away from this point of initial impact and causes the formation of an oval disk, while, simultaneously, supplying molten liquid into the disk.

We consider two sets of cylindrical coordinates $O(r,\theta,z)$ and $O'(r',\theta',z)$. The origin O of the first set is placed at the impact point, with r and θ on the substrate surface and z extending perpendicularly upward. The origin O' of the other set is the second focal point that is moving with the particle as shown in **Fig. 2**. If we are on the moving coordinates $O'(r',\theta',z)$ and observe the particle flattening, the particle does not apparently move laterally and the liquid from the particle flows out radially into the spreading disk. Thus the r' component $u_{r'}$ of the flow field $U'(u_{r'},u_{\theta'},u_{z'})$ in the splat is assumed as follows;

$$u_{r'} = C_1 v_0 \sin\varphi \cdot e^{-\alpha t} z(2h-z)r', \quad r' < R_0 \tag{1}$$

$$u_{r'} = C_2 v_0 \sin\varphi \cdot e^{-\alpha t} \frac{z(2h-z)}{r'}, \quad r' \geq R_0 \tag{2}$$

where C_1, C_2 and α are constants that are determined by initial and boundary conditions, and $R_0 \approx d_0/2$ [5,6]. The θ' and z components in $U'(u_{r'},u_{\theta'},u_{z'})$ can be negligible because their velocity gradient is negligibly small since the flattening disk is too thin in comparison with its radius. When r' in the moving coordinates is expressed in the original coordinates r and θ, the next equation holds;

$$r' = \left(r\cos\theta - r_p\right)^2 + r^2 \sin^2\theta \tag{3}$$

The term r_p is the distance between the two origins of the two sets of coordinates and also between the first

and the second focal points in the ellipse. We assume that r_p is

$$r_p = 2k = \int_0^t v_0 \cos\varphi \cdot e^{-n\alpha t} dt = \frac{v_0 \cos\varphi}{n\alpha}\left(1 - e^{-n\alpha t}\right) \quad (4)$$

where "n" is a constant and $0 < n \leq 1$, and "k" is the focal length of the ellipse. The second focal point moves at velocity $v_0 \cos\varphi$ at impact and the velocity decreases with time because the term $\exp(-n\alpha t)$ decreases rapidly with increasing time.

If the droplet supplies all its liquid into the spreading oval disk and the liquid flows out through the area around the moving focal point whose radius and thickness are R_0 and h respectively, then, the liquid volume of the oval splat from time $t = 0$ to t equals the volume that flows out through the boundary $r' = R_0$ for the same time range. Then;

$$\int_0^t dt \int_0^{2\pi} \frac{1}{2} hR^2 d\theta - \pi h R_0^2 = \int_0^t dt \int_0^{2\pi} \int_0^h u_r R_0 dz d\theta' \quad (5)$$

where "R" is the elliptic radius from the initial focal point that is the impact point. The elliptic curve is expressed as,

$$R = \frac{g \cdot e}{1 - e\cos\theta} \quad (6)$$

where g is a constant and is expressed as,

$$g = \frac{a_m^2\left(1 - \frac{k_m^2}{a_m^2}\right)}{k_m} \quad (7)$$

where a_m is the long radius of the splat that stops its spreading just when it loses its kinetic energy and k_m is the focal length in the final oval splat, and "e" is eccentricity. e is defined as,

$$e = \frac{k}{a} = \sqrt{\frac{k}{g + k}} \quad (8)$$

where "a" and "k" are the elliptic long radius and focal length of the splat at time t, respectively.

The term "α" is determined by solving equation (5), and C_1 and C_2 are determined by the procedure shown in a previous study [5,6]. α is a factor that shows how the particle is decelerated when the droplet moves down onto the substrate. On the other hand, $\exp(-n\alpha t)$ in equation (4) is also the deceleration factor of lateral motion. The term "$n\alpha$" is used instead of just α since the lateral speed of the droplet on the flattening disk is decelerated less than that in the perpendicular direction, since sliding motion has a smaller resistance than that of vertical motion. A lower value of "n" indicates lower resistance and indicates a more elongated ellipse.

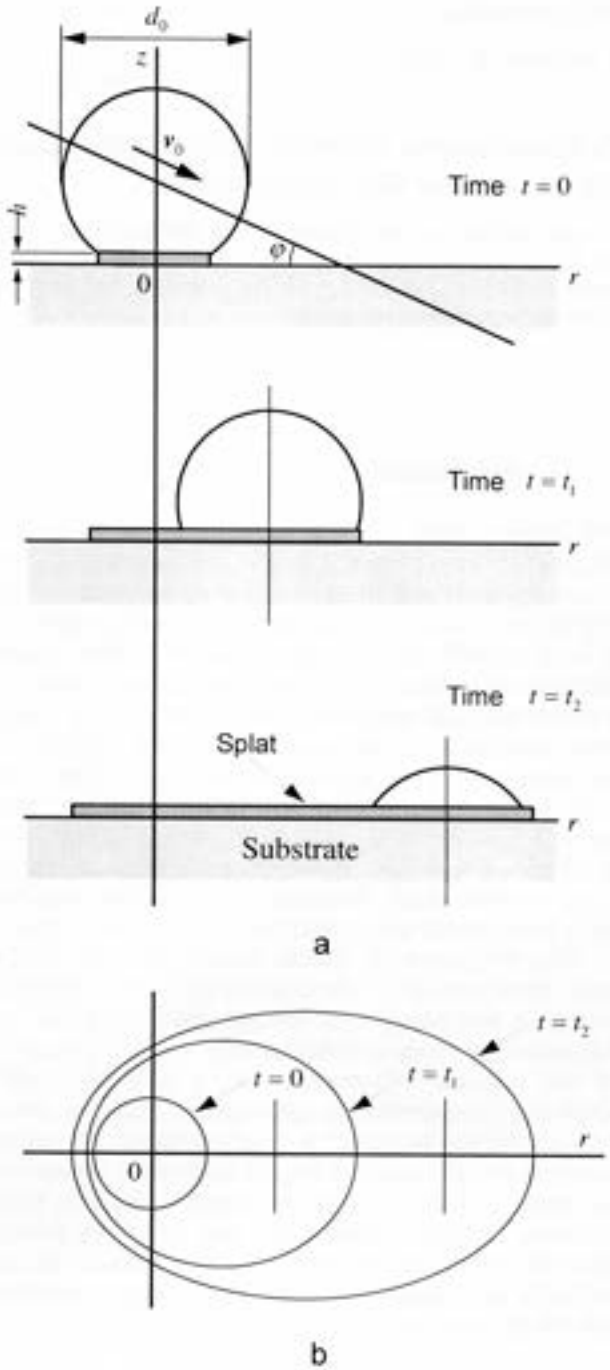

a

b

Fig. 1 Schematic flattening processes of impact droplet at off-normal angles.
Fig. 1-a side view, b overhead view

The area of the elliptic shaped splat is determined by solving the equation of energy dissipation by friction in the splat that is equal to the kinetic energy that the droplet holds at impingement. When the kinetic energy of the impact particle is E_k, then,

$$E_k = \int_0^\infty dt \int_v \mu \left(\frac{\partial u_r}{\partial z}\right)^2 dV \quad (9)$$

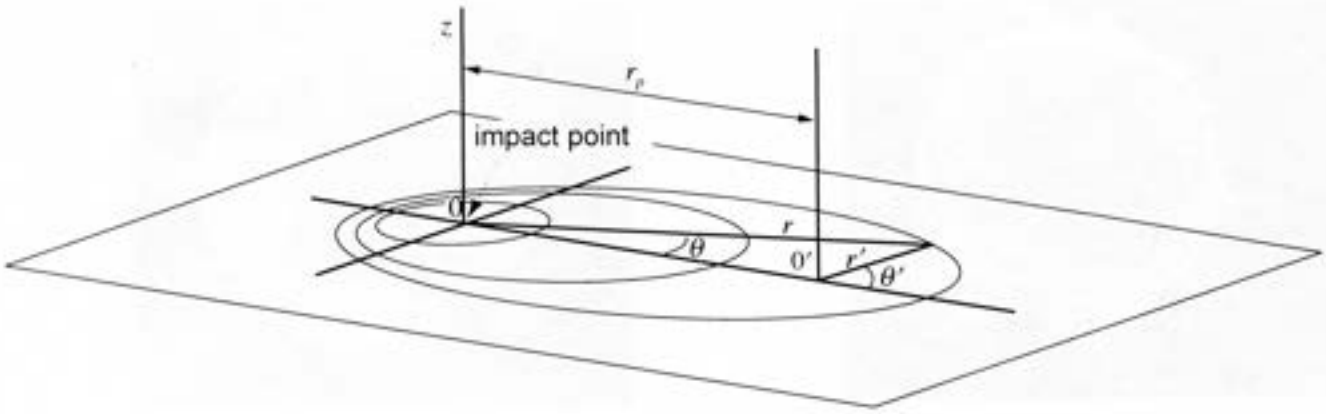

Fig. 2 Illustration of relationship between static and moving coordinates.

where "μ" is the viscous coefficient of the droplet liquid and "V" is the volume of the flattening disk at time t.

3. Experimental Procedure and Results

3.1 Experimental Procedure

Copper and nickel powders were sprayed in Xian Jiaotong University and Plasma Giken, respectively.

Copper powder whose particle sizes ranged from 74 to 88 μm was sprayed onto a stainless steel substrate with a plasma torch. The substrates were preheated to 250°C on the back side. Shielding plates were fixed in front of the substrates to obtain splats with minimal errors of angle. Spray angle φ was changed from 60° to 90° in 5° steps. Argon and hydrogen gas were used as the arc gas and input current and voltage were 400 A and 60 V, respectively. The powder was fed into the plasma jet vertically upward.

Nickel powder ranging from -100 to +325 mesh was sprayed onto a stainless steel substrate by a plasma torch using argon and helium as the arc gas. Arc current and voltage were 800 A and 35 V, respectively. The substrates were preheated to 350°C on the back side. The spray angle was changed from 15° to 90° in 15° steps.

3.2 Experimental Results

Sprayed copper and nickel splats were collected and photographed. The typical morphology of copper and nickel splats are shown in **Fig. 3** and **Fig. 4**, respectively. Splat diameters were measured choosing ten samples of copper and one splat of nickel at each angle. The ratio of the long diameter to its orthogonal short diameter was calculated for each.

The Cu and Ni splats at spray angles more than 60° are almost circles. The Cu and Ni splats at spray angles greater than 45° exhibit two different parts that are the central and outer areas. The elongation ratio of the central area is smaller than that of the entire splat. In the photographs, the splat surfaces of the central sections are smooth and the peripheral areas are roughened.

The Ni splats at 30° and 15° look splashed because the peripheral sections were not observed. Thus, the real elongation ratios could be larger than those of the photographs.

4. Comparison of The Model to The Experimental Results

From the model, the elongation ratio ER of the splats is defined by the following equation.

$$ER = \frac{a_m}{\sqrt{a_m^2 - k_m^2}} \tag{10}$$

ER is determined by substituting k_m into equation (10) which is solved from equation (4) and (5) as a function of radius a_m of the splat and impinging angle φ. Then;

$$ER = \frac{1}{\sqrt{1 - \dfrac{-1 + \sqrt{1 + 576n^4 \tan^4 \varphi}}{288n^4 \tan^4 \varphi}}} \tag{11}$$

The results of the experiment and the model are shown in **Fig. 5**.

The graph shows that the experimental data agree quite well with the theoretical curve. Although the data near the normal angle are larger than the predicted values, this arrives from measurement error because the splats are not ideal ellipses and the peripheral curves are not smooth. As well, the elongation ratio is close to 1 due to the spray angle being nearly perpendicular.

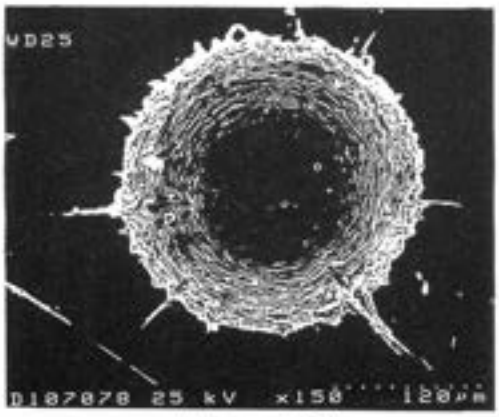

φ = 90° ×150

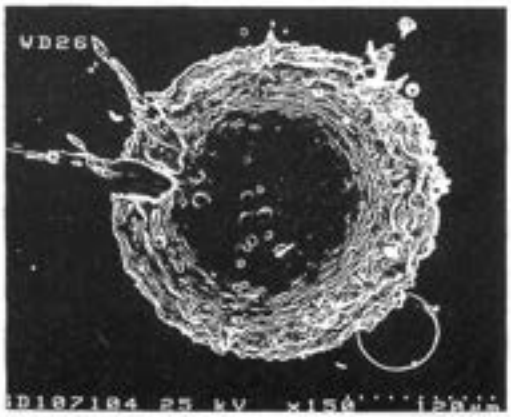

φ = 70° ×150

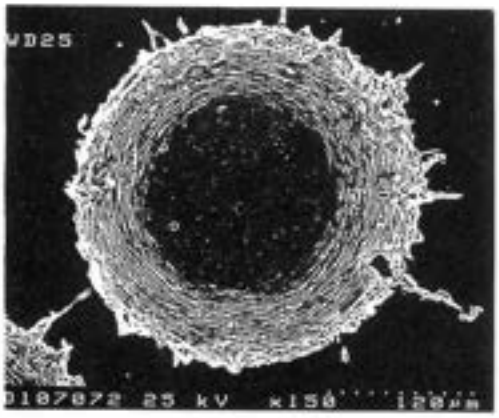

φ = 85° ×150

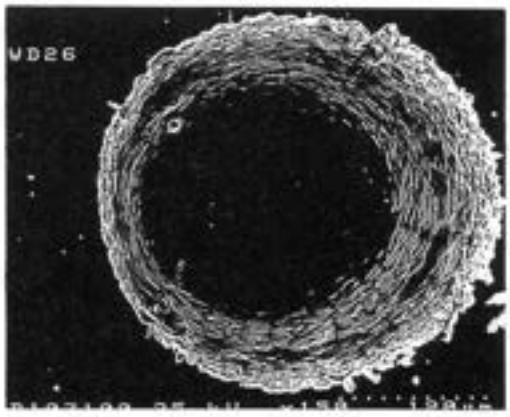

φ = 65° ×150

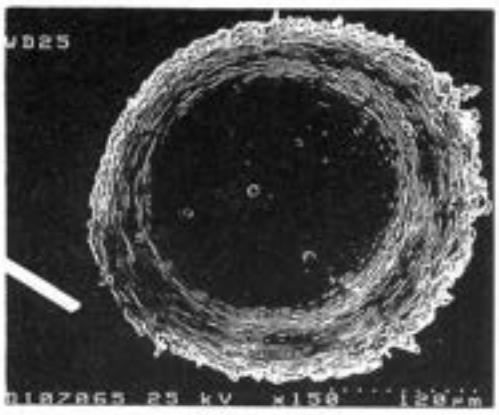

φ = 80° ×150

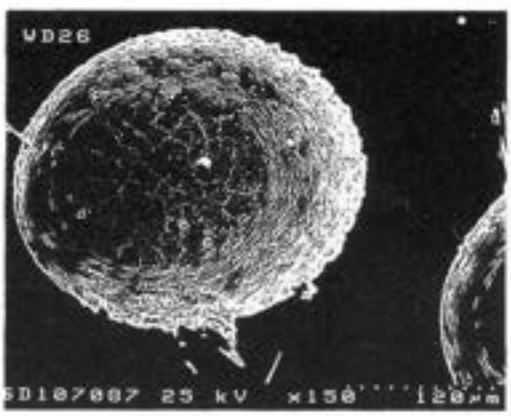

φ = 60° ×150

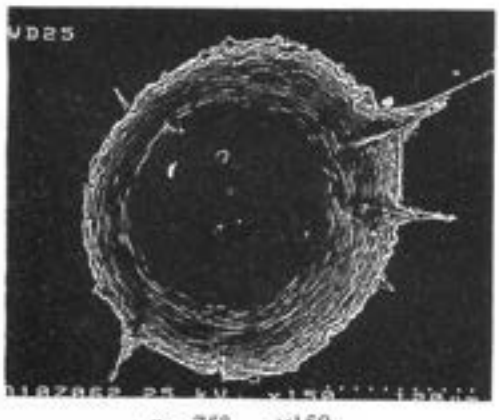

φ = 75° ×150

Fig. 3 Morphology of Cu splats at spray angles from 60° to 90°

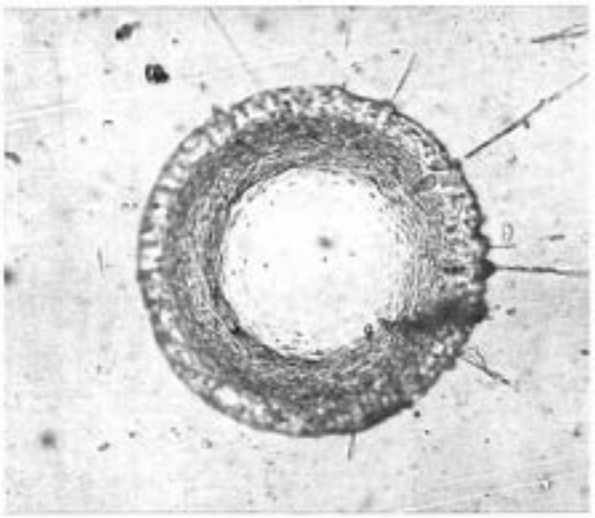

$\varphi = 90°$ ×400

$\varphi = 45°$ ×400

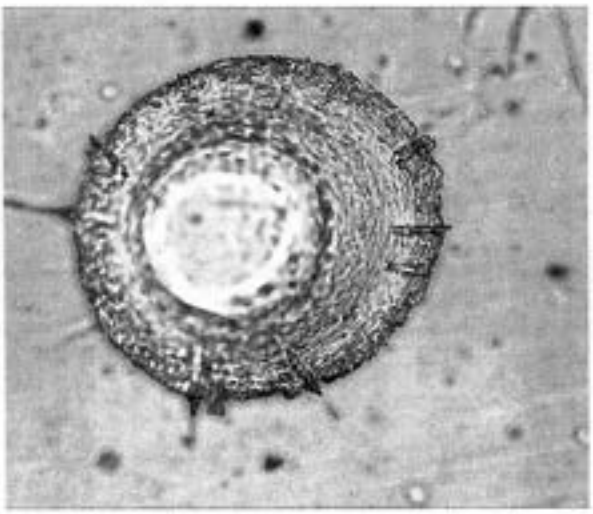

$\varphi = 75°$ ×400

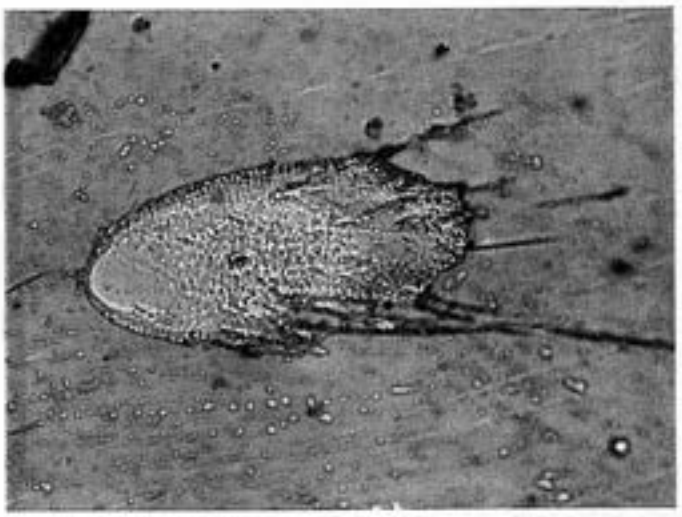

$\varphi = 30°$ ×400

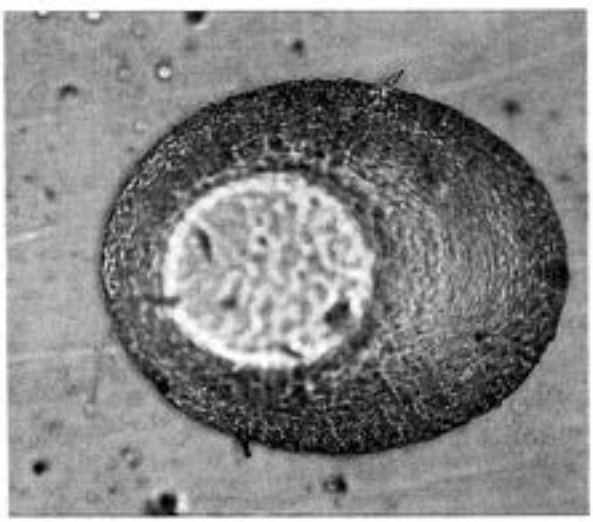

$\varphi = 60°$ ×400

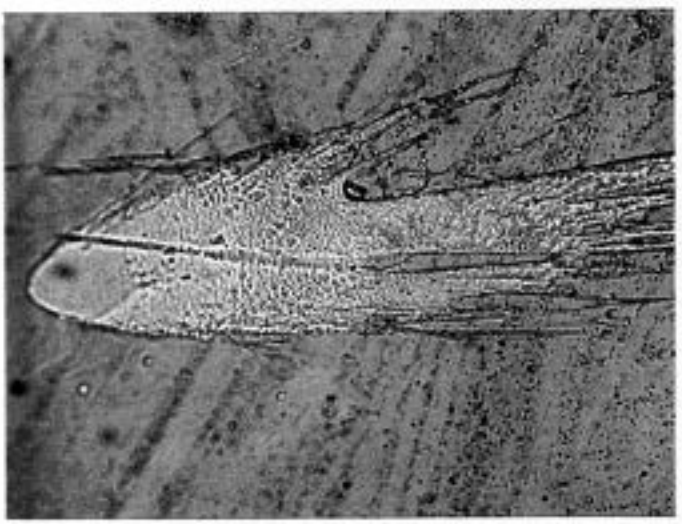

$\varphi = 15°$ ×400

Fig. 4 Morphology of Ni splats at spray angles from 15° to 90°

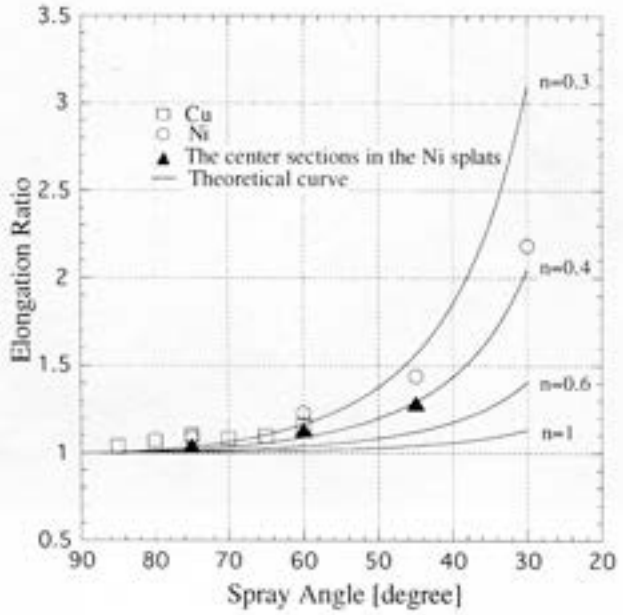

Fig. 5 Elongation ratios of experimental results and the model.

5. Conclusions

The results of the experiment show that the elongation ratio increases with an increasing inclined spray angle, and that the model can predict the relation between the elongation ratio and the spray angle.

We need experiments on other spray materials and under more varied conditions to clarify the processes of the off-normal spray angles and to confirm the model adaptability.

6. Literature

[1] G. Montavan, C. Coddet S. Sampath H. Herman, C. C. Berndt: Vacuum Plasma Spray Forming of Astroloy: An Investigation of Processing Parameters, Proceedings of the 7th Thermal Spray Conference, Boston, 20-24 June, 1994, pp. 469-475.

[2] G. Montavan and C. Coddet: 3-D Profilometries of Vacuum Plasma Sprayed Nickel-Based Alloy Splats Using Scanning Mechanical Microscopy, Proceedings of the 8th National Thermal Spray Conference, Houston, 11-15 September 1995, pp. 285-289.

[3] M. F. Smith, R. A. Neiser and R. C. Dykhuizen: An Investigation of the Effects of Droplet Impact Angle In Thermal Spray Deposition, Proceedings of the 7th National Thermal Spray Conference, Boston, 20-24 June 1994, pp. 603-608.

[4] V. V. Sobolev and J. M. Guilemany: Droplet Flattening Thermal Spraying at Off-Normal Angles, Proceedings of the 15th International Thermal Conference, Nice, France, 25-29 May 1998, pp. 497-502.

[5] H. Fukanuma: A Porosity Formation and Flattening Model of an Impinging Molten Particle in Thermal Spray Coatings, Journal of Thermal Spray Technology, Vol. 3 (1) March (1994), pp. 33-44.

[6] H. Fukanuma and A. Ohmori: Behavior of Molten Droplets Impinging on Flat Surfaces, Proceedings of the 7th National Thermal Spray Conference, Boston, 20-24 June 1994, pp. 563-568.